Application of the Grid Convergency Index Method and Courant Number Analysis for Propeller Turbine Simulation

Dendy Adanta[1,*], Mochammad Malik Ibrahim[2], Dewi Puspita Sari[3], Imam Syofii[3], Muhammad Amsal Ade Saputra[1]

[1] Department of Mechanical Engineering, Faculty of Engineering, Universitas Sriwijaya, Indralaya 30662, South Sumatera, Indonesia
[2] Study Program of Geological Engineering, Faculty of Engineering, Universitas Sriwijaya, Indralaya 30662, South Sumatera, Indonesia
[3] Study Program of Mechanical Engineering Education, Faculty of Teacher Training and Education, Universitas Sriwijaya, Indralaya 30662, South Sumatera, Indonesia

ARTICLE INFO	ABSTRACT
	The computational method has long been used in propeller turbine studies. However, there has not yet been a comprehensive explanation for mesh and timestep independency method or verification for propeller turbine simulation. Hence, this study explains propeller turbines' mesh and timestep independency method. The computational software for this case is ANSYS® FLUENT 18.2™. The grid convergence index (GCI) and the Courant number (C_n) analysis determine the optimum mesh and timestep size. Based on the results, the mesh number of 691996 (medium) is considered appropriate in this case because the GCI is below 1%. The 691996 mesh has a size (Δx) of 0.432 mm. The C_n is 0.72 (the water velocity of 0.63 m/s) based on the investigation; therefore, the timestep size for this case of 0.0005s. Then, verification of the CFD results in the propeller turbine can be indicated by visualising the pressure contour; the pressure on the upper side of the runner should be higher than the lower side. The deviation average of CFD results in secondary data of 14.48%. The deviation is presumably because of missed information about the CFD setup geometry with real conditions. Thus, the independency method using the GCI method and C_n analysis is recommended for propeller turbines. CFD results show that torque, power generated, and efficiency of the propeller turbine toward its rotation have a similar pattern to secondary data; it can indicate that the CFD results of the propeller turbine are verified.

1. Introduction

Propeller turbines are reaction turbines where the energy absorbed is kinetic and pressure [1–3]. The propeller turbine is often used as a power plant because of its stable efficiency due to the wide specific speed (N_s) range of 300 to 1000 m-kW [4]. The Ns for the turbine is a function of turbine rotation (n), head (h), and power [5]. The Ns is a non-dimensional number that aims to determine a condition's turbine dimension [6]. The propeller turbine is similar to the Kaplan turbine, where propeller turbines have a fixed blade while the Kaplan turbines do not [4, 6]. Since the Kaplan turbine

has an adjustable blade, it is desirable for mini scales to the top. In contrast, propeller turbine is in demand for microscale to the below [8].

The development of technology makes computational methods interesting in studying the propeller turbine [8-9]; since the computational methods can describe the physical phenomenon more than experimental and analytical [11]. Therefore, converting energy from fluid to runner is well understood [12].

Studies examining propeller turbines using computational methods have been carried out. Adanta *et al.,* [13] studied the effect of gaps between blades on the energy conversion process. Simulation from computational methods describes the flow field in the propeller turbine in detail and precision [13]. The computational results visualise changes in fluid velocity vector due to wide gaps between blades [13]. Warjito *et al.,* [14] investigated the transfer of energy on flat and aerofoil blades in propeller turbines. Computational results can visualise the difference in pressure on the upper and lower blade [14]. Based on results, for propeller turbines with small-scale such as pico hydro (< 5 kW), a flat blade is recommended [8, 13] since the production of lift and drag force by aerofoil blade is not significant [14]. Then, the comprehensive CFD method for propeller turbine is done by Cifuentes *et al.,* [9]. Cifuentes *et al.,* [9] compared the inflation layers around the blade and concluded that it affects the CFD results. Hence the mesh quality should be considered for propeller turbine simulation. Ramos *et al.,* [15] evaluated the propeller turbine performance using the CFD method. Ramos *et al.,* [15] recommended the CFD method as verificatory first the propeller turbine performance.

Furthermore, the feasibility study propeller pump applied as a turbine was done using the CFD method [16]. Based on the results, CFD can be applied to predicting propeller turbine of pump performance [16]. A study of the integrated CFD method to the electrical generator for propeller turbine to predict the power losses were done by Borkowski *et al.,* [17]. In addition, Borkowski *et al.,* [17] studied the effect of the turbulence model on power losses prediction. Based on the results, the k-ε standard can predict power losses in propeller turbines [17]. Then, the CFD method was used to calculate the propeller turbine performance by changing the flow rate and the number of blades [18]. The advantage of the CFD method is that it can study the flow field more comprehensively than experiments [19]. Hence the analysis aerodynamics small scale blade propeller turbine mostly uses the CFD method [20]. The CFD results can be used as a reference to determine the appropriate shape and angle of the aerofoil to increase the lift runner force [20].

Although the computational method has long been used in propeller turbine studies, there has not yet been a comprehensive explanation for mesh and timestep independency method or verification for propeller turbine simulation. Hence, this study explains propeller turbines' mesh and timestep independency method. The computational software for this case is ANSYS® FLUENT 18.2™. The grid convergency index (GCI) [20-21] and the Courant number (C_n) analysis [19] are used to determine the optimum mesh and timestep size.

2. Methodology
2.1 CFD Method

The simulation has three stages: pre-processing, processing, and post-processing. This study only describes pre-processing step. The pre-processing activity is divided into three parts [9]: import geometry from computer-aided design (CAD) software to Ansys Fluent, meshing process, and setup of simulation or defining boundary conditions [23].

The turbine geometry used is from Warjito *et al.,* [24], and as validator is Ho-Yan study's [25]. The detailed geometry: the number of blades (z) is 4, outer diameter (d1) of 130 mm, inner diameter (d2)

of 70 mm, angle of attack at the inlet ($\alpha 1$) of 34.8°, stagger angle (ζ) of 73.7°, blade angle at the inlet ($\beta 1$) of 72.4°, angle of attack at the outlet ($\alpha 2$) of 7.5°, blade angle at the outlet ($\beta 2$) of 74.9°, inlet diameter (D1) of 141.3 mm, outlet diameter (D2) of 298.06 mm, and draft tube height (t) of 1.7 m. The visualisation of the geometry in Figure 1.
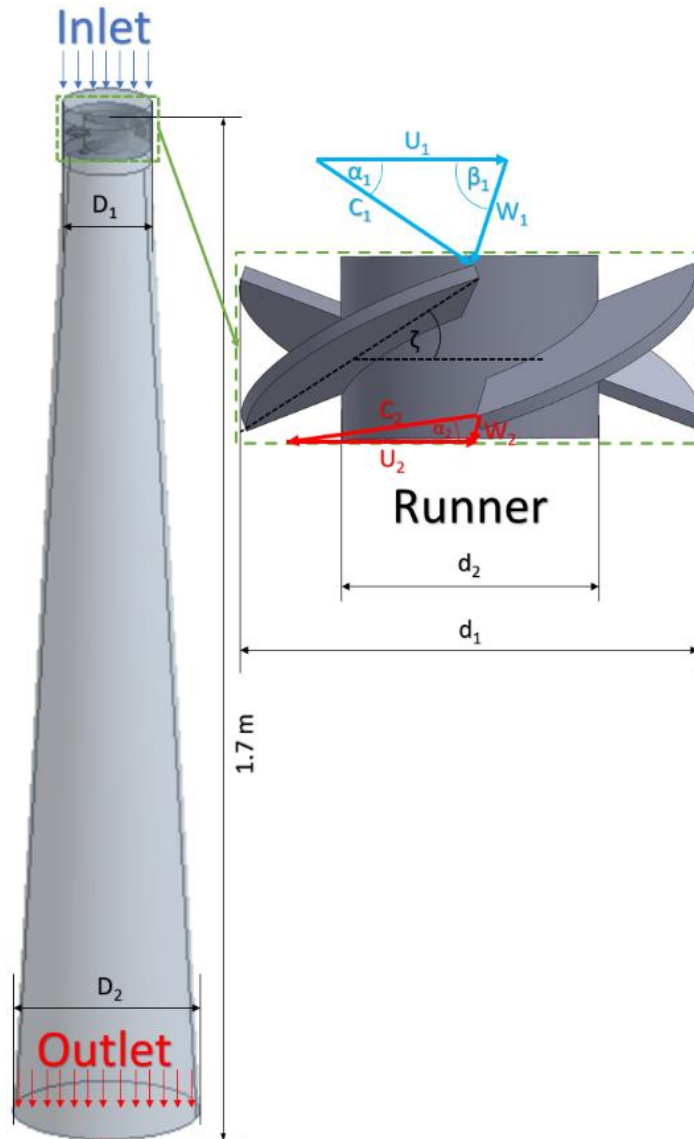
Fig. 1. Schematic of propeller turbine

ANSYS® FLUENT 18.2™ was used for computational calculations. Three-dimensional (3D) analysis using six degrees of freedom (6-DoF) features was applied due to the complex shape of the propeller blades. The 6-DoF feature was chosen because the rotation is an independent variable; the rotation depends on the mass flow of fluid hitting the blade [24-25]. Pressure-based solver is applied because the fluid flow is incompressible (water) [19] with a transient approach (timestep). Therefore, the mass conservation and momentum conservation equation become [26-27]

$$\frac{\partial(\rho)}{\partial t} + \frac{\partial(\rho u_j)}{\partial x_j} = 0 \tag{1}$$

$$\frac{\partial(\rho u_i)}{\partial t} + \frac{\partial(\rho u_i u_j)}{\partial x_j} = -\frac{\partial p}{\partial x_i} + \frac{\partial(\tau_{ij} - \rho u_i' u_j')}{\partial x_j} + \rho g_i \tag{2}$$

where p is pressure, τ_{ij} is shear stress, and $-\rho u_i'u_j'$ is Reynolds stress. $-\rho u_i'u_j'$ is calculated based on the Reynolds Average Navier-Stokes (RANS) viscous model; the turbine propeller flow is expected to occur in turbulence [11]. $-\rho u_i'u_j'$ becomes [28-29]

$$-\rho u_i' u_j' = \mu_t \left(\frac{\partial u_i}{\partial x_j} + \frac{\partial u_j}{\partial x_i}\right) - \frac{2}{3}\left(\rho k + \mu_t \frac{\partial u_i}{\partial x_i}\right)\delta_{ij} \tag{3}$$

Therefore, the Reynolds Average Navier-Stokes (RANS) viscous model based on two equations of the k-ε standard is applied for this case. The k-ε standard can represent fluid phenomena with reasonably good accuracy [9, 30]. The standard k–ε equation is [33]
For k:

$$\frac{\partial(\rho k)}{\partial t} + \frac{\partial(\rho k u_i)}{\partial x_j} = \frac{\partial}{\partial x_i}\left(\left(\mu + \frac{\mu_t}{\sigma_k}\right)\frac{\partial k}{\partial x_j}\right) + G_k + G_b + \rho\varepsilon + Y_M + S_k \tag{4}$$

For ε

$$\frac{\partial(\rho\varepsilon)}{\partial t} + \frac{\partial(\rho\varepsilon u_i)}{\partial x_j} = \frac{\partial}{\partial x_i}\left(\left(\mu + \frac{\mu_t}{\sigma_\varepsilon}\right)\frac{\partial\varepsilon}{\partial x_j}\right) + C_{1\varepsilon}\frac{\varepsilon}{k}(G_k + C_{3\varepsilon}G_b) - C_{2\varepsilon}\rho\frac{\varepsilon^2}{k} + S_\varepsilon \tag{5}$$

2.2 Independency Test Method

The torque generated by the runner is the parameter used for the mesh number test—the mesh number test using grid convergency index (GCI) analysis. The GCI calculates the error of each mesh number against the exact value ($\tau_{\to\infty}$) [20-21]. $\tau_{\to\infty}$ is the extrapolation by torque fine mesh (τ_f), torque medium mesh (τ_m), and torque coarse mesh (τ_c). Therefore, the analysis error of each mesh number becomes

$$\mathrm{GCI}_{fm} = F_s \left|\frac{1}{\tau_f}\frac{\tau_m - \tau_f}{r_{fm}{}^{q_n} - 1}\right| \times 100\% \tag{6}$$

where F_s is the safety factor or estimation tolerance of 1.25, r is the grid refinement ratio of $r_{fm}=(m_f/m_m)^{0.5}$. m is the number of mesh. Then, q_n is obtained from numerical calculations using analysis

$$q_{n+1} = \ln\left|\left(\frac{\tau_c - \tau_m}{\tau_m - \tau_f}\left(r_{fm}{}^{q_n-1}\right)\right) + r_{fm}{}^{q_n}\right| / \ln\left(r_{fm} \times r_{mc}\right) \tag{7}$$

The initial value for Eq. (7) of 2. Then, the $\tau_{\to\infty}$ is calculated using the extrapolation approach

$$\tau_{\to\infty} = \tau_f - \left(\frac{\tau_m - \tau_f}{r_{fm}^{\,q_n+1} - 1} \right) \tag{8}$$

Further, analysis of the normalised grid spacing (h) is done using Eq. (8). The example of Eq. (8) analysis is

$$h_{cm} = \frac{2}{r_{cm}}; h_{mf} = \frac{r_{cm}}{r_{fm}} \tag{9}$$

For the timestep size (Δt), the calculation of the independency test is recommended to use the Courant number (Cn) [19]. The Cn is a non-dimensional analysis that visualises particle fluid passing through a mesh; ideally, C_n of 1 [19]. The Cn is more than 1 considered the particle uncalculated in the mesh (particles skip a cell) [19]. The calculation of C_n is

$$C_n = u_i \times \frac{\Delta t}{\Delta x} \tag{10}$$

3. Results and Discussion
3.1 GCI Calculation Results

The minimum elements number for GCI analysis is three [20-21, 32]. There are three elements number verified: 318,306 (coarse), 691,996 (medium), and 1,460,865 (fine). Therefore, r_{fm} of 1.453 and r_{mc} of 1.474. Forward, using Eq. 9, h for coarse of 2, medium of 1.36, and fine of 0.93. The h for $\tau_{\to\infty}$ of 0; 0 is assumed ∞.

Torque of each mesh number of: 0.806 N·m (coarse); 0.835 N·m (medium); and 0.839 N·m (fine). Then, the numerical calculation for q_n using Eq. (7). Based on the numerical calculation, the q_n of 5.0694. Further, the extrapolation of $\tau_{\to\infty}$ using Eq. (8) was based on the calculation $\tau_{\to\infty}$ of 0.84 N·m. Next, GCI analysis using Eq. (6). GCI analysis shows that the fine mesh has 0.1%, a medium of 0.7%, and a coarse of 2.67%. Figure 2 is the relation of torque and GCI to h.

Based on Figure 2(a), the mesh number of 691,996 (medium) is considered appropriate in this case because the GCI is below 1%. The visualisation of the 691,996 mesh can be seen in Figure 2(b).
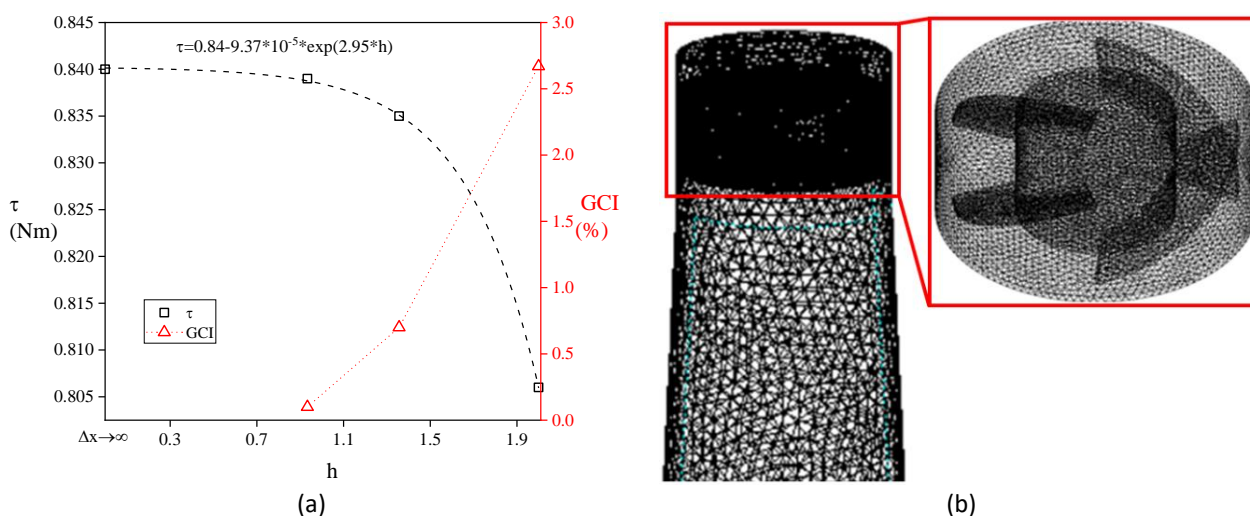
Fig. 2. Mesh Independency test results (a) GCI Results (b) 691996 mesh visualisation

3.2 C_n Calculation Results

There are three timesteps size (Δt) was compared: 0.0025s (1000 Hz), 0.001s (2500Hz), and 0.0005s (5000 Hz). The 691996 mesh has a size (Δx) of 0.432 mm. The probe water velocity at coordinate 0.2,0,0. The investigation location is 0.2 m from the inlet and in the centre of the tube. Based on the investigation, the water velocity of 0.63 m/s. Table 1 is the result of calculations using Eq. 1 with these data. Based on Table 1, the Δt for this case of 0.0005s (5000Hz).

Table 1
C_n calculation results

Parameters	Value
Δt	0.0025s; 0.001s; 0.0005s
Δx	0.432 mm
u_i	0.63 m/s
C_n	3.62; 1.45; 0.72

3.3 Validation of Works

Figure 3(a) is the relation of torque (τ) to the rotational speed; the relation is linear. Based on Figure 3(a), the τ increases the n decreases. τ CFD results in the Ho-Yan study [25] have the same pattern (Figure 3(a)). Figure 3(b) is the relation of power mechanic (P_{mech}) and efficiency (η) to n; the relation is parabolic. Based on Figure 3(b), the maximum η and P_{mech} occur at 200 rpm; this condition is similar to the case of Ho-Yan [25]; this work adapts Ho-Yan's study [25]. The relation in Figure 3 is similar to previous works [12, 33] and in other turbines such as the Turgo turbine [36], Pelton turbine [37], and breastshot waterwheel [38]. Based on Figure 3, the deviation average of CFD results in the Ho-Yan study [25] is 14.48%. Therefore, the CFD results are verified.
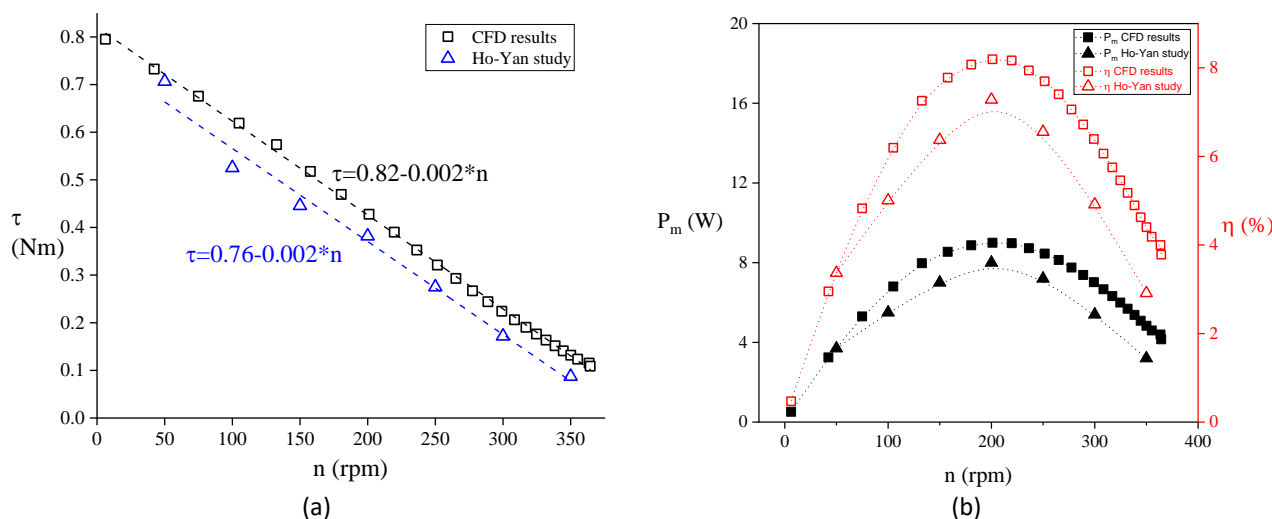
Fig. 3. Comparison of CFD results to Ho-Yan study [25] (a) τ to n (b) P_m to n

Figure 4 is a visualisation of the pressure contour of the CFD results. Based on Figure 4, a pressure gradient occurs between the upper and lower sides of the runner. The upper side runner has a higher pressure than the lower. The visualisation of the pressure contour of the CFD results in Figure 4 is similar to the Adanta *et al.,* study [13]. Based on Bernoulli's principle, the water velocity on the upper side is lower than on the lower side. Based on Figure 4, the draft tube works well and indicates that the CFD results follow real conditions. The low pressure on the lower side is necessary because the

runner needs the suction effect. The suction effect is generated due to low pressure on the lower side, increasing the runner torque. Hence the draft tube should be placed below the water level; otherwise, the draft tube pressure returns to atmospheric pressure. Therefore, the visualisation of the pressure contour shown in Figure 4 can indicate verification of the CFD results in the propeller turbine.
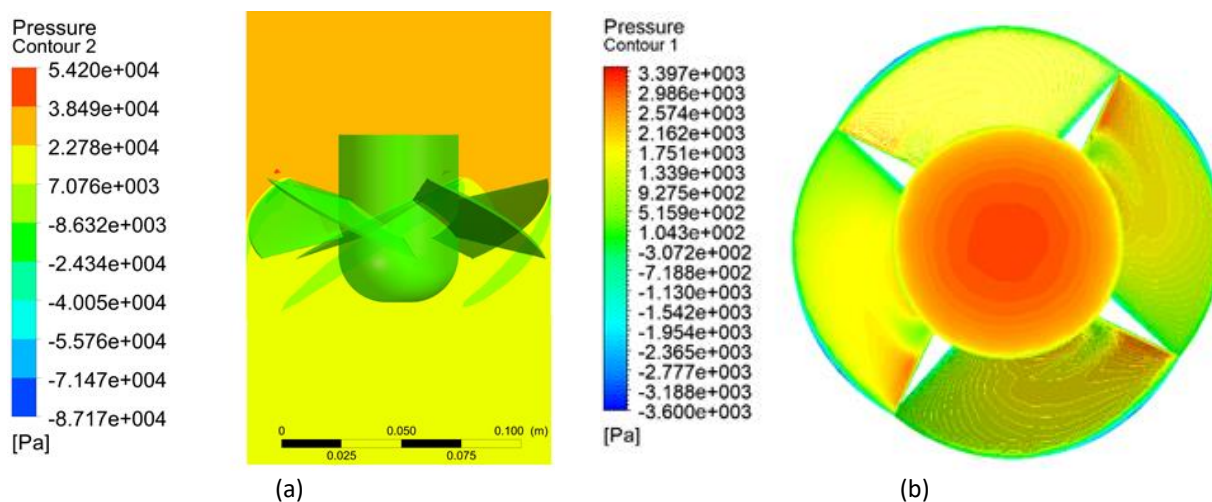
Fig. 3. Visualisation of pressure contour at 200 rpm (a) Front view (b) Top view

4. Conclusions

This study explains propeller turbines' mesh and timestep independency method. The computational software for this case is ANSYS® FLUENT 18.2™. The grid convergency index (GCI) [20-21] are used to determine the optimum mesh, and the Courant number (C_n) analysis [19] for timestep size. Based on the results, the independency method using the GCI method and C_n analysis is recommended for propeller turbines. CFD results show that torque, power generated, and efficiency of the propeller turbine toward its rotation have a similar pattern to secondary data; it can indicate that the CFD results of the propeller turbine are verified. The deviation average of CFD results in secondary data of 14.48%. The 14% deviation is presumably because of missed information about the CFD setup geometry with real conditions; because the validator uses secondary data. In addition, the reference study [25] does not explain in detail the uncertainty and error of the measuring instrument.

References
[1] Khattak, M. A., NS Mohd Ali, NH Zainal Abidin, N. S. Azhar, and M. H. Omar. "Common Type of Turbines in Power Plant: A Review." *Journal of Advanced Research in Applied Sciences and Engineering Technology* 3, no. 1 (2016): 77-100.
[2] Basar, Mohd Farriz, Nurul Ashikin M. Rais, Azhan Ab Rahman, Wan Azani Mustafa, Kamaruzzaman Sopian, and Kaifui V. Wong. "Optimization of Reaction Typed Water Turbine in Very Low Head Water Resources for Pico Hydro." *Journal of Advanced Research in Fluid Mechanics and Thermal Sciences* 90, no. 1 (2022): 23-39. https://doi.org/10.37934/arfmts.90.1.2339
[3] Nechleba, Miroslav. *Hydraulic turbines, their design and equipement*. No. BOOK. Artia, 1957.

[4]   Syah, Ardian. "Manual Pembangunan PLTMH-Tri Mumpuni." *Jakarta: Japan International Cooperation Agency* (2017).

[5]   Harinaldi, Budiarso. "Sistem Fluida Prinsip Dasar dan penerapan Mesin Fluida, Sistem Hidrolik, dan Sistem Penumatik." *Jakarta: Erlangga* (2015).

[6]   Nasution, Sanjaya Baroar Sakti, Warjito Warjito, Budiarso Budiarso, and Dendy Adanta. "A comparison of openflume turbine designs with specific speeds (Ns) based on power and discharge functions." *Journal of Advanced Research in Fluid Mechanics and Thermal Sciences* 51, no. 1 (2018): 53-60.

[7]   Darsono, Febri Budi, Rahmad Doni Widodo, and Akhmad Nurdin. "Analysis Of the Effect of Flow Rate and Speed on Four Blade Tubular Water Bulb-Turbine Efficiency Using Numerical Flow Simulation." *Journal of Advanced Research in Fluid Mechanics and Thermal Sciences* 90, no. 2 (2021): 1-8. https://doi.org/10.37934/arfmts.90.2.18

[8]   Chica Arrieta, Edwin Lenin, Sergio Agudelo Flórez, and Natalia Isabel Sierra. "Application of CFD to the design of the runner of a propeller turbine for small hydroelectric power plants." *Revista Facultad de Ingeniería Universidad de Antioquia* 69 (2013): 181-192.

[9]   Cifuentes, Oscar Darío Monsalve, Jonathan Graciano Uribe, and Diego Andrés Hincapié Zuluaga. "Numerical Simulation of a Propeller-Type Turbine for In-Pipe Installation." *Journal of Advanced Research in Fluid Mechanics and Thermal Sciences* 83, no. 1 (2021): 1-16. https://doi.org/10.37934/arfmts.83.1.116

[10]   Adanta, Dendy, Sanjaya BS Nasution, Budiarso, Warjito, Ahmad Indra Siswantara, and Havel Trahasdani. "Open flume turbine simulation method using six-degrees of freedom feature." In *AIP Conference Proceedings*, vol. 2227, no. 1, p. 020017. AIP Publishing LLC, 2020. https://doi.org/10.1063/5.0004389

[11]   Adanta, Dendy, Budiarso Budiarso, and Ahmad Indra Siswantara. "Assessment of turbulence modelling for numerical simulations into pico hydro turbine." *Journal of Advanced Research in Fluid Mechanics and Thermal Sciences* 46, no. 1 (2018): 21-31.

[12]   Siswantara, Ahmad Indra, Budiarso Budiarso, Aji Putro Prakoso, Gun Gun R. Gunadi, Warjito Warjito, and Dendy Adanta. "Assessment of turbulence model for cross-flow pico hydro turbine numerical simulation." *CFD Letters* 10, no. 2 (2018): 38-48.

[13]   Adanta, Dendy, Emanuele Quaranta, and T. M. I. Mahlia. "Investigation of the effect of gaps between the blades of open flume Pico hydro turbine runners." *Journal of Mechanical Engineering and Sciences* 13, no. 3 (2019): 5493-5512. https://doi.org/10.15282/jmes.13.3.2019.18.0444

[14]   Warjito, Sanjaya BS Nasution, Dendy Adanta, Budiarso, and Ahmad Indra Siswantara. "Comparison of plate and aerofoil blade performance in open-flume turbines." In *AIP Conference Proceedings*, vol. 2227, no. 1, p. 020020. AIP Publishing LLC, 2020. https://doi.org/10.1063/5.0001620

[15]   Ramos, Helena M., Mariana Simão, and A. Borga. "Experiments and CFD analyses for a new reaction microhydro propeller with five blades." *Journal of Energy Engineering* 139, no. 2 (2013): 109-117. https://doi.org/10.1061/(ASCE)EY.1943-7897.0000096

[16]   Derakhshan, Shahram, and Nemat Kasaeian. "Optimization, numerical, and experimental study of a propeller pump as turbine." *Journal of Energy Resources Technology* 136, no. 1 (2014). https://doi.org/10.1115/1.4026312

[17]   Borkowski, Dariusz, Michał Węgiel, Paweł Ocłoń, and Tomasz Węgiel. "CFD model and experimental verification of water turbine integrated with electrical generator." *Energy* 185 (2019): 875-883. https://doi.org/10.1016/j.energy.2019.07.091

[18]   Park, Ji-Hoon, You-Taek Kim, Yong Cho, Byeong-Kon Kim, and Young-Ho Lee. "Performance analysis of 10kW class propeller hydro turbine by the change of flow rates and the number of runner vane using CFD." *The KSFM Journal of Fluid Machinery* 17, no. 2 (2014): 5-11. https://doi.org/10.5293/kfma.2014.17.2.005

[19]   Fluent, A. N. S. Y. S. "Release 15.0, theory guide." *ANSYS Inc, Canonsburg* (2013).

[20]   Loureiro, Eric Vargas, Nicolas Lima Oliveira, Patricia Habib Hallak, Flávia de Souza Bastos, Lucas Machado Rocha, Rafael Grande Pancini Delmonte, and Afonso Celso de Castro Lemonge. "Evaluation of low fidelity and CFD methods for the aerodynamic performance of a small propeller." *Aerospace Science and Technology* 108 (2021): 106402. https://doi.org/10.1016/j.ast.2020.106402

[21]   Roache, Patrick J. *Verification and validation in computational science and engineering*. Vol. 895. Albuquerque, NM: Hermosa, 1998.

[22]   Roache, Patrick J. "Quantification of uncertainty in computational fluid dynamics." *Annual review of fluid Mechanics* 29, no. 1 (1997): 123-160. https://doi.org/10.1146/annurev.fluid.29.1.123

[23]   Alfarawi, Suliman SS, Azeldin El-sawi, and Hossin Omar. "Exploring Discontinuous Meshing for CFD Modelling of Counter Flow Heat Exchanger." *Journal of Advanced Research in Numerical Heat Transfer* 5, no. 1 (2021): 26-34.

[24]   Syahputra, Muhammad Farhan, and Sanjaya BS Nasution. "The effect of blades gap on propeller open-flume picohydro turbine performance." *International Journal of Fluid Machinery and Systems* 14, no. 1 (2021): 122-131. https://doi.org/10.5293/IJFMS.2021.14.1.122

[25] Ho-Yan, Bryan. "Design of a low head pico hydro turbine for rural electrification in Cameroon." PhD diss., University of Guelph, 2012.

[26] Adanta, Dendy, Richiditya Hindami, and Ahmad Indra Siswantara. "Blade depth investigation on cross-flow turbine by numerical method." In *2018 4th International Conference on Science and Technology (ICST)*, pp. 1-6. IEEE, 2018. https://doi.org/10.1109/ICSTC.2018.8528291

[27] Prakoso, Aji Putro, Warjito Warjito, Ahmad Indra Siswantara, Budiarso Budiarso, and Dendy Adanta. "Comparison Between 6-DOF UDF and Moving Mesh Approaches in CFD Methods for Predicting Cross-Flow PicoHydro Turbine Performance." *CFD Letters* 11, no. 6 (2019): 86-96.

[28] Khalil, Hesham, Khalid Saqr, Yehia Eldrainy, and Walid Abdelghaffar. "Aerodynamics of a trapped vortex combustor: A comparative assessment of RANS based CFD models." *Journal of Advanced Research in Fluid Mechanics and Thermal Sciences* 43, no. 1 (2018): 1-19.

[29] Alfarawi, Suliman. "Evaluation of hydro-thermal shell-side performance in a shell-and-tube heat exchanger: CFD approach." *Journal of Advanced Research in Fluid Mechanics and Thermal Sciences* 66, no. 1 (2020): 104-119.

[30] Rahman, Tariq Md Ridwanur, Waqar Asrar, and Sher Afghan Khan. "An Investigation of RANS Simulations for Swirl-Stabilized Isothermal Turbulent Flow in a Gas Turbine Burner." *CFD Letters* 11, no. 9 (2019): 14-31.

[31] Hakim, Muhammad Luqman, Bagus Nugroho, Rey Cheng Chin, Teguh Putranto, I. Ketut Suastika, and I. Ketut Aria Pria Utama. "Drag penalty causing from the roughness of recently cleaned and painted ship hull using RANS CFD." *CFD Letters* 12, no. 3 (2020): 78-88. https://doi.org/10.37934/cfdl.12.3.7888

[32] Adanta, Dendy, Muhamad Agil Fadhel Kurnianto, and Sanjaya BS Nasution. "Effect of the number of blades on undershot waterwheel performance for straight blades." In *IOP Conference Series: Earth and Environmental Science*, vol. 431, no. 1, p. 012024. IOP Publishing, 2020. https://doi.org/10.1088/1755-1315/431/1/012024

[33] Yusuf, Siti Nurul Akmal, Yutaka Asako, Nor Azwadi Che Sidik, Saiful Bahri Mohamed, and Wan Mohd Arif Aziz Japar. "A short review on rans turbulence models." *CFD Letters* 12, no. 11 (2020): 83-96. https://doi.org/10.37934/cfdl.12.11.8396

[34] Warjito, Warjito, Budiarso Budiarso, Celine Kevin, Dendy Adanta, and Aji Putro Prakoso. "Computational methods for predicting a pico-hydro crossflow turbine performance." *CFD Letters* 11, no. 12 (2019): 13-20.

[35] Warjito, Warjito, Sanjaya BS Nasution, Muhammad Farhan Syahputra, Budiarso Budiarso, and Dendy Adanta. "Study of turbulence model for performance and flow field prediction of pico hydro types propeller turbine." *CFD Letters* 12, no. 8 (2020): 26-34. https://doi.org/10.37934/cfdl.12.8.2634

[36] Williamson, Sam J., Bernard H. Stark, and Julian D. Booker. "Performance of a low-head pico-hydro Turgo turbine." *Applied Energy* 102 (2013): 1114-1126. https://doi.org/10.1016/j.apenergy.2012.06.029

[37] Gupta, Vishal, Vishnu Prasad, and Ruchi Khare. "Numerical simulation of six jet Pelton turbine model." *Energy* 104 (2016): 24-32. https://doi.org/10.1016/j.energy.2016.03.110

[38] Quaranta, Emanuele, and Roberto Revelli. "Hydraulic behavior and performance of breastshot water wheels for different numbers of blades." *Journal of Hydraulic Engineering* 143, no. 1 (2017): 04016072. https://doi.org/10.1061/(ASCE)HY.1943-7900.0001229